

Molecular Hydrogen Formation from Photocatalysis of Methanol on Anatase-TiO₂(101)

Chenbiao Xu,^{†,‡,§} Wenshao Yang,^{†,§} Qing Guo,^{†,*} Dongxu Dai,[†] Maodu Chen,[‡] and Xueming Yang^{†,*}

[†]State Key Laboratory of Molecular Reaction Dynamics, Dalian Institute of Chemical Physics, 457 Zhongshan Road, Dalian 116023, Liaoning, P. R. China

[‡]School of Physics and Optoelectronic Engineering, Dalian University of Technology, 2 Linggong Road, Dalian 116024, China

S Supporting Information

ABSTRACT: Photocatalysis of methanol (CH₃OH) on anatase (A)-TiO₂(101) has been investigated using temperature programmed desorption (TPD) method with 266 nm light at low surface temperatures. Experimental results show that CH₃OH adsorbs on the A-TiO₂(101) surface predominantly in molecular form, with only a small amount of CH₃OH in dissociated form. Photocatalytic products, formaldehyde (CH₂O) and methyl formate (HCOOCH₃), have been detected under 266 nm light irradiation. In addition to H₂O formation, H₂ product is also observed by TPD spectroscopy. Experimental results indicate that H₂ product is formed via thermal recombination of H-atoms on the BBO sites from photocatalysis of CH₃OH on the A-TiO₂(101) surface, and H₂ production on the A-TiO₂(101) surface is significantly more efficient than that on the rutile (R)-TiO₂(110) surface.

Titanium dioxide, TiO₂, is a widely used material with important applications in many areas, particularly in heterogeneous catalysis, gas sensors, and electronic devices and biomaterials.^{1–8} TiO₂ exists in three polymorphs: rutile, anatase, and brookite. Rutile and anatase TiO₂ materials have been often used in the study of hydrogen (H₂) production from photocatalytic water splitting,^{9–11} as well as degradation of organic pollutants.¹² Despite lots of work focusing on rutile (R)-TiO₂, the anatase form is the most active polymorph in commercial applications for catalysis actually.⁵ A previous study found that adding methanol (CH₃OH) to pure water solution can dramatically enhance H₂ production, implying that CH₃OH played a crucial role in H₂ production.¹³ In recent years, photocatalysis of CH₃OH on TiO₂ has been extensively studied as a benchmark system.^{2,14–23} Elementary processes in CH₃OH photocatalysis on the R-TiO₂(110) surface have been clarified. Most recently,²⁴ we have shown that D₂ can be formed via thermal recombination of dissociated D-atoms on the bridge-bonded oxygen (BBO) sites from photocatalysis of fully deuterated CH₃OH, suggesting that the last molecular D₂ formation step on the R-TiO₂(110) surface is a thermally driven process. Since only about 7% of D-atoms on the BBO sites contribute to D₂ formation with most D-atoms recombining with BBO atoms to form D₂O, it implies that H₂ formation is not the most efficient process on the R-TiO₂(110) surface. Even though a lot of photocatalysis studies have been carried out on anatase

(A)-TiO₂ particles, very little was done on well-defined surfaces. Thus far, only a few experimental studies of thermal chemistry on A-TiO₂(101) have been carried out,^{25–30} and photocatalytic chemistry on this well-defined surface has not been investigated at all. In this work, we have investigated molecular H₂ formation on A-TiO₂(101) from photocatalysis of CH₃OH using temperature programmed desorption (TPD) and time-of-flight (TOF) methods, in combination with laser surface photocatalysis. Our results show that H₂ is formed via thermal recombination of dissociated H-atoms on the BBO sites from photocatalysis of CH₃OH on A-TiO₂(101). In addition, we found that H₂ formation on A-TiO₂(101) is considerably more efficient than on R-TiO₂(110).²⁴

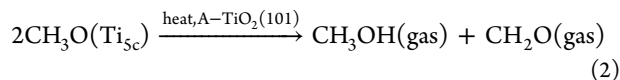
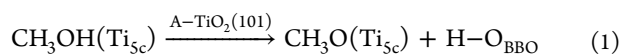
The surface photocatalysis-TPD apparatus used in this work has been described previously in detail.^{22,31} The base pressure of the sample chamber is $<6 \times 10^{-11}$ Torr. A highly sensitive quadrupole mass spectrometer (QMS) (Extrel) is used to detect TPD and TOF products from the surface. An extremely high vacuum of 1.5×10^{-12} Torr was achieved and maintained in the electron-impact ionization region. The A-TiO₂(101) ($6 \times 1 \text{ mm}^3$, Princeton Scientific Corp.) surface was prepared by cycles of Ar⁺ sputtering and resistive heating to 800 K in vacuum until all impurities were removed. CH₃OH (Aldrich, 99.9%) purified by several freeze/pump/thaw cycles was introduced to the A-TiO₂(101) surface with a calibrated molecular beam doser. The 266 nm light used to irradiate the TiO₂ surface came from a frequency tripled Ti:Sapphire femtosecond laser (repetition rate 1 kHz, pulse duration ~ 70 fs). About a 20 mW laser light beam with a diameter of 3 mm was directed at the sample surface at an angle of $\sim 30^\circ$ from the surface parallel. The photo flux impinging on the surface is 1.9×10^{17} photons $\text{cm}^{-2} \text{ s}^{-1}$. The TPD spectrum after a certain time of laser irradiation was measured with a heating rate of 2 K/s, with the surface directly pointing to the mass spectrometer. In addition, TOF measurements for certain photodesorbed products were also made during laser irradiation.

Before investigating the photocatalytic chemistry of CH₃OH, TPD spectra of CH₃OH on the A-TiO₂(101) surface as a function of coverage were measured (Supporting Information (SI) Figure S1). Five desorption features peaked at 142 K, 188 K, 270 K, 410 K, and 650 K are observed, similar to previous results with slightly better resolution.²⁹ A 650 K peak is also observed in TPD spectra at $m/z = 30, 31, \text{ and } 32$ (SI Figure S2). This is likely

Received: October 28, 2013

Published: December 30, 2013

due to methoxy (CH_3O) disproportionation at the five-coordinated $\text{Ti}^{4+}(\text{Ti}_{5c})$ sites, as on the $\text{R-TiO}_2(110)$ surface,²¹



where O_{BBO} is bridge bonded oxygen and the coverage of $\text{CH}_3\text{O}(\text{Ti}_{5c})$ from $m/z = 30$ and 31 TPD is calculated to about 0.02 ML. The fact that the 650 K peak in $m/z = 30$ and 31 TPD decreases rapidly after 5 s of irradiation while the 300 K peak changes little implies that CH_3O has a much higher reactivity than molecular CH_3OH on this surface (Figure 1A and B). This is consistent with previous studies by Shen and Henderson on $\text{R-TiO}_2(110)$.²¹

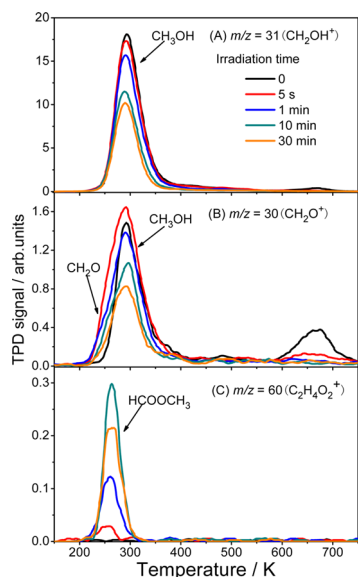
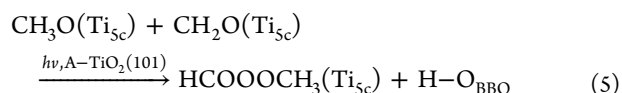
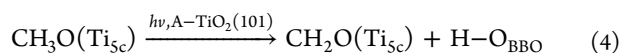
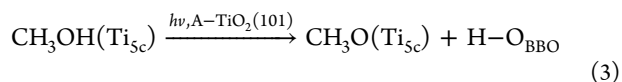


Figure 1. 0.38 ML of CH_3OH were dosed to the $\text{A-TiO}_2(101)$ surfaces at 100 K. (A) Typical TPD spectra collected at $m/z = 31$ (CH_2OH^+) as a function of irradiation time with a photon flux of 1.9×10^{17} photons $\text{cm}^{-2} \text{s}^{-1}$. CH_2OH^+ is mainly formed by dissociative ionization of the desorbed parent CH_3OH molecule in the electron-bombardment ionizer. (B) Typical TPD spectra collected at $m/z = 30$ (CH_2O^+) as a function of irradiation time. The $m/z = 30$ (CH_2O^+) signal has two components: the parent ion signal of formaldehyde (CH_2O), as well as the ion-fragment signals of the parent CH_3OH molecule. (C) Typical TPD spectra collected at $m/z = 60$ ($\text{C}_2\text{H}_4\text{O}_2^+$) as a function of irradiation time. The $m/z = 60$ ($\text{C}_2\text{H}_4\text{O}_2^+$) signal is from the parent ion signal of HCOOCH_3 molecule.

We then carried out a systematic study on the photocatalytic chemistry of 0.38 ML of CH_3OH covered $\text{A-TiO}_2(110)$ surface using 266 nm light with different irradiation times. As shown in Figure 1A, the 290 K peak at TPD spectra of $m/z = 31$ (CH_2OH^+), which is assigned to molecular CH_3OH desorption from Ti_{5c} sites, decreases as irradiation time increasing, suggesting that CH_3OH on the $\text{A-TiO}_2(101)$ surface has been photocatalytically dissociated. Photocatalytic products, formaldehyde (CH_2O at $m/z = 30$) and methyl formate (HCOOCH_3 at $m/z = 60$), have been clearly detected with different laser irradiation times (Figure 1B and C). Meanwhile, TOF signals of CH_2O ($m/z = 30$) and CH_3OH ($m/z = 32$) were monitored during laser irradiation (SI Figure S3). The intensity of the TOF signal at $m/z = 30$ is about 4 times larger than that at $m/z = 32$,

and whereas the cracking signal of CH_3OH to $m/z = 30$ is only $1/5$ of the parent mass ion signal in our quadrupole mass detector (SI Figure S4), the fact that the TOF signal at $m/z = 30$ is considerably larger implies that the TOF signal at $m/z = 30$ should mostly come from photodesorbed CH_2O on Ti_{5c} sites. These observed products are similar to that on the $\text{R-TiO}_2(110)$ surface.³² The photocatalytic mechanisms for the formation of these products are also believed to be similar to that on the $\text{R-TiO}_2(110)$ surface. The most likely mechanism of CH_2O formation is via transferring the hydroxyl H and a methyl group H of CH_3OH to the O_{BBO} sites nearby, while the product HCOOCH_3 is likely formed through a cross coupling reaction of CH_2O and CH_3O , similar to that on the $\text{R-TiO}_2(110)$ surface.³² The formation of HCOOCH_3 is an indirect evidence of the existence of $\text{CH}_3\text{O}(\text{Ti}_{5c})$.



In these processes, dissociated H atoms are transferred to the O_{BBO} sites. It is thus interesting to see how molecular H_2 is formed from these dissociated H atoms.

To detect dissociated H-atoms from photocatalysis of CH_3OH on the $\text{A-TiO}_2(101)$ surface, we have measured TPD spectra at different masses. Figure 2A shows TPD spectra at $m/z = 18$

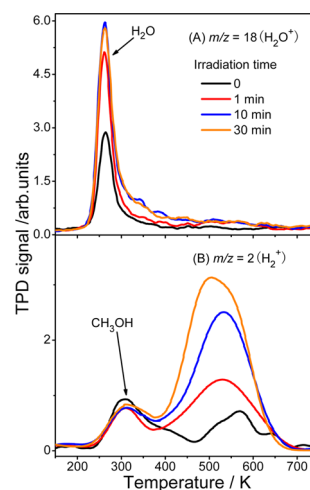


Figure 2. TPD spectra collected at $m/z = 2$ and 18 , from photocatalysis of 0.38 ML of CH_3OH covered $\text{A-TiO}_2(101)$ at 100 K with a photon flux of 1.9×10^{17} photons $\text{cm}^{-2} \text{s}^{-1}$.

(H_2O^+) after different irradiation durations with 0.38 ML of CH_3OH covered $\text{A-TiO}_2(101)$ surface. Before irradiation, a rather sharp peak at $m/z = 18$ is observed near 260 K. This is assigned to H_2O desorption from Ti_{5c} sites. No obvious H_2O desorption signal was detected at higher temperature, suggesting that there are nearly no point defects on the surface. A recent study shows that only about 0.005 ML of point defects on the $\text{A-TiO}_2(101)$ surface could be formed by annealing.³³ However, the amount of desorbed H_2O observed here corresponds to about 0.025 ML, which is about 6.6% of all CH_3OH adsorbed on

the surface. This could not be attributed to the impurity of H₂O in the CH₃OH sample, which is <0.6%, according to our measurement on the R-TiO₂(110) surface using the same CH₃OH sample. Thus, the desorbed H₂O at 260 K must come from some thermal reactions during the TPD process. In addition, a broad TPD peak from 400 to 700 K was also detected at $m/z = 15$ (SI Figure S5). The direct desorption of CH₃ radical could be related to the H₂O TPD desorption at 260 K. From these results, we propose that the H₂O TPD peak at 260 K is due to the following thermally driven exchange reaction (Figure 3):

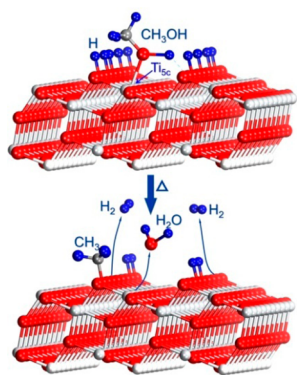
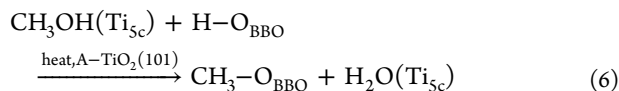


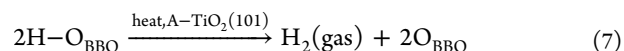
Figure 3. Schematic diagram of the mechanism of molecular H₂ production from H–O_{BBO} on a A-TiO₂(101) surface.

This is similar to previous experimental observations.³⁴ The original HO_{BBO} species here should come from the small amount of dissociatively adsorbed CH₃OH on the surface. Furthermore, the TOF signal of CH₃ (SI Figure S3) from likely CH₃–O_{BBO} was also detected, consistent with the above picture. As more H–O_{BBO} species are formed from photocatalysis of CH₃OH on the A-TiO₂(101) surface, the H₂O TPD peak increases (Figure 2A). The intensity of the H₂O TPD peak reaches a maximum after 10 min of laser irradiation. However, the photoinduced H₂O signal is only slightly larger than that without laser irradiation, suggesting that the H₂O formation process is not enhanced significantly by photocatalysis.

As shown above, some H–O_{BBO} species are depleted by exchanging with CH₃ groups in CH₃OH so that H₂O will be formed. Molecular H₂ may be formed by recombination of H–O_{BBO} as in the case of R-TiO₂(110).²⁴ It is thus interesting to know the relative importance of molecular H₂ formation versus H₂O formation on the A-TiO₂(101) surface, since this could relate to the efficiency of H₂ production. In the case of CD₃OD photocatalysis on the R-TiO₂(110) surface, D₂O formation is much more important than D₂ formation (see SI Figure S6), suggesting that H₂ formation is less efficient. Indeed, when we have attempted to detect H₂ product from photocatalysis of CH₃OH on R-TiO₂(110), no signal was detected.

To determine if molecular H₂ product could be formed, TPD spectra at $m/z = 2$ (H₂⁺) were measured after 266 nm laser irradiation, as shown in Figure 2B. There are two main sources of signals at $m/z = 2$. Clearly, the TPD peak at about 300 K comes from the fragmentation of desorbed molecular CH₃OH in the ionizer. Another obvious source is the H₂ product formed via recombinative desorption of H–O_{BBO}. As indicated in Figure 2B,

the TPD peak near 550 K is most likely due to this source and is strongly dependent on the laser irradiation time. When the surface temperature is above 400 K, CH₂O, CH₃OH, HCOOCH₃, and H₂O on A-TiO₂(101) have all been desorbed, and CH₃O_{BBO}, HO_{BBO}, and CH₃O(Ti⁴⁺) are the only three species left. Obviously, CH₃O(Ti⁴⁺) is mostly depleted after laser irradiation for only 1 min. No evidence of any other larger molecules on the surface is observed during TPD measurements. The contribution of the fragmentation from CH₃ radical at $m/z = 2$ is quite small before irradiation. After 30 min irradiation, the intensity of the CH₃ radical peak only increases by about 2 times (SI Figure S5). Thus, we can conclude that the 550 K TPD desorption peak at $m/z = 2$ arises mainly from the recombination of H atoms at O_{BBO} sites (Figure 3):



We have also attempted to detect H₂ product during laser irradiation and no signal was detected, indicating that H₂ formation is a thermally driven recombination process, not a photodriven reaction. From the above results and our previous studies,²⁴ it is clear that molecular H₂ formation from photocatalysis of CH₃OH on A-TiO₂(101) occurs via photocatalytic dissociation of CH₃OH followed by thermal recombination of H–O_{BBO}, similar to that on R-TiO₂(110).

We now evaluate the relative importance of H₂ formation in comparison to H₂O formation on A-TiO₂(101). To do that, the yields of H₂O and H₂ products as a function of laser irradiation time have been measured and plotted in Figure 4. The yields of

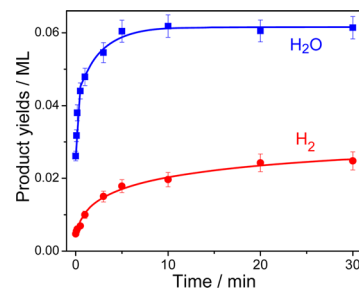


Figure 4. Yields of the molecular H₂, H₂O TPD products as a function of laser irradiation time.

H₂O and H₂ products shown in Figure 4 have already been calibrated based on the detection efficiencies of the two products in the quadrupole mass detector. The result of the current measurement shows that 0.025 ML of H₂ and 0.035 ML of H₂O are formed after 30 min of irradiation. This indicates that the H₂ formation channel is nearly as important as the H₂O formation process on the A-TiO₂(101) surface. This result is significantly different from that on the R-TiO₂(110) surface. On the R-TiO₂(110) surface, we have shown that the D₂O formation process is about 13 times more efficient than the molecular D₂ formation process.²⁴ It is interesting to note that the H₂O TPD signal reaches maximum at 10 min while the H₂ TPD signal continues to grow up at 30 min on the A-TiO₂(101) surface. In addition, the H₂O formation mechanisms are also quite different for the two surfaces. We have attempted to measure the TOF signal of O-atom from a bare A-TiO₂(101) surface when irradiated with UV light, and no measurable O-atom TOF signal was detected, suggesting that no surface defects are created during UV irradiation and the O_{BBO} atoms are very stable. This is likely the reason that dissociated H atoms at the O_{BBO} sites

mostly come off as H₂ on the A-TiO₂(101) surface, not taking an O_{BBO} to form H₂O (Figure 3). Thus, if there is the same amount of H-atoms on the BBO sites, molecular H₂ formation on the A-TiO₂(101) surface should be more efficient than that on the R-TiO₂(110) surface.

In present study, relatively monochromatic UV light is used to study photocatalysis on a well characterized surface in ultrahigh vacuum, while most photocatalysis studies use particle photocatalysts under bulk conditions and discharge lamps that also contain UV light. The purpose of the current study is to try to understand the underlying elementary photocatalytic processes, which are difficult to probe in bulk experiments.

UV photocatalysis of CH₃OH on a well-defined A-TiO₂(101) surface has been investigated using TPD and TOF methods. Experimental results show unambiguously that molecular H₂ formation from UV photocatalysis of CH₃OH on the A-TiO₂(101) surface is a thermally driven process that occurs via H-atom recombination on the O_{BBO} sites and is clearly not a photodriven process. More interestingly, we found that formation of molecular H₂ and H₂O are comparable on the A-TiO₂(101) surface, while formation of molecular H₂ on R-TiO₂(110) is much less efficient than H₂O. This suggests that the H₂ formation process should be more efficient on the A-TiO₂(101) surface relative to the R-TiO₂(110) surface. The present investigation of the mechanism of H₂ formation from UV methanol photocatalysis on A-TiO₂(101) could also help us to understand the nature of H₂ production on TiO₂ photocatalysts.

■ ASSOCIATED CONTENT

Supporting Information

Yield and characterization details. This material is available free of charge via the Internet at <http://pubs.acs.org>.

■ AUTHOR INFORMATION

Corresponding Author

guoqing@dicp.ac.cn, xmyang@dicp.ac.cn

Author Contributions

[§]C.X. and W.Y. made similar contributions to this work.

Notes

The authors declare no competing financial interest.

■ ACKNOWLEDGMENTS

This work was supported by the Chinese Academy of Sciences, National Science Foundation of China (20923002), and the Chinese Ministry of Science and Technology (2013CB834605).

■ REFERENCES

- (1) Hoffmann, M. R.; Martin, S. T.; Choi, W. Y.; Bahnemann, D. W. *Chem. Rev.* **1995**, *95*, 69–96.
- (2) Thompson, T. L.; Yates, J. T., Jr. *Chem. Rev.* **2006**, *106*, 4428–4453.
- (3) Henderson, M. A.; Otero-Tapia, S.; Castro, M. E. *Faraday Discuss.* **1999**, *114*, 313–319.
- (4) Gong, X.-Q.; Selloni, A.; Dulub, O.; Jacobson, P.; Diebold, U. *J. Am. Chem. Soc.* **2008**, *130*, 370–381.
- (5) Henderson, M. A. *Surf. Sci. Rep.* **2011**, *66*, 185–297.
- (6) Pang, C. L.; Lindsay, R.; Thornton, G. *Chem. Soc. Rev.* **2008**, *37*, 2328–2353.
- (7) Fujishima, A.; Zhang, X.; Tryk, D. *Surf. Sci. Rep.* **2008**, *63*, 515–582.
- (8) Diebold, U. *Surf. Sci. Rep.* **2003**, *48*, 53–229.
- (9) Henrich, V. E.; Dresselhaus, G.; Zeiger, H. *J. Phys. Rev. Lett.* **1976**, *36*, 1335–1339.
- (10) Lo, W. J.; Chung, Y. W.; Somorjai, G. A. *Surf. Sci.* **1978**, *71*, 199–219.

- (11) Schwitzgebel, J.; Ekerdt, J. G.; Gerischer, H.; Heller, A. *J. Phys. Chem.* **1995**, *99*, 5633–5638.
- (12) Zang, L.; Lange, C.; Abraham, I.; Storck, S.; Maier, W. F.; Kisch, H. *J. Phys. Chem. B* **1998**, *102*, 10765–10771.
- (13) Kawai, T.; Sakata, T. *J. Chem. Soc., Chem. Commun.* **1980**, *15*, 694–695.
- (14) Farfan-Arribas, E.; Madix, R. J. *Surf. Sci.* **2003**, *544*, 241–260.
- (15) Bates, S. P.; Gillan, M. J.; Kresse, G. *J. Phys. Chem. B* **1998**, *102*, 2017–2026.
- (16) Onda, K.; Li, B.; Zhao, J.; Petek, H. *Surf. Sci.* **2005**, *593*, 32–37.
- (17) Sadeghi, M.; Liu, W.; Zhang, T.-G.; Stavropoulos, P.; Levy, B. *J. Phys. Chem.* **1996**, *100*, 19466–19474.
- (18) Yamakata, A.; Ishibashi, T.; Onishi, H. *J. Phys. Chem. B* **2002**, *106*, 9122–9125.
- (19) Li, B.; Zhao, J.; Onda, K.; Jordan, K. D.; Yang, J.; Petek, H. *Science* **2006**, *311*, 1436–1440.
- (20) Zhou, C.; Ren, Z.; Tan, S.; Ma, Z.; Mao, X.; Dai, D.; Fan, H.; Yang, X.; LaRue, J.; Cooper, R.; Wodtke, A. M.; Wang, Z.; Li, Z.; Wang, B.; Yang, J.; Hou, J. *Chem. Sci.* **2010**, *1*, 575–580.
- (21) Shen, M.; Henderson, M. A. *J. Phys. Chem. Lett.* **2011**, *2*, 2707–2710.
- (22) Guo, Q.; Xu, C.; Ren, Z.; Yang, W.; Ma, Z.; Dai, D.; Fan, H.; Minton, T. K.; Yang, X. *J. Am. Chem. Soc.* **2012**, *134*, 13366–13373.
- (23) Kavan, L.; Gratzel, M.; Gilbert, S. E.; Klemenz, C.; Scheel, H. J. *J. Am. Chem. Soc.* **1996**, *118*, 6716–6723.
- (24) Xu, C.; Yang, W.; Guo, Q.; Dai, D.; Yang, X. *J. Am. Chem. Soc.* **2013**, *135*, 10206–10209.
- (25) Diebold, U.; Ruzycski, N.; Herman, G. S.; Selloni, A. *Catal. Today* **2003**, *85*, 93–100.
- (26) Shklover, V.; Nazeeruddin, M.-K.; Zakeeruddin, S. M.; Barbé, C.; Kay, A.; Haibach, T.; Steurer, W.; Hermann, R.; Nissen, H.-U.; Grätzel, M. *Chem. Mater.* **1997**, *9*, 430–439.
- (27) Tilocca, A.; Selloni, A. *Langmuir* **2004**, *20*, 8379–8384.
- (28) Hebenstreit, W.; Ruzycski, N.; Herman, G. S.; Gao, Y.; Diebold, U. *Phys. Rev. B* **2000**, *62*, R16334. Gong, X.-Q.; Sellon, A.; Batzill, M.; Diebold, U. *Nat. Mater.* **2006**, *5*, 665–670.
- (29) Herman, G. S.; Dohnálek, Z.; Ruzycski, N.; Diebold, U. *J. Phys. Chem. B* **2003**, *107*, 2788–2795.
- (30) Zehr, R. T.; Henderson, M. A. *Surf. Sci.* **2008**, *602*, 1507–1516.
- (31) Ren, Z.; Guo, Q.; Xu, C.; Yang, W.; Xiao, C.; Dai, D.; Yang, X. *Chin. J. Chem. Phys.* **2012**, *5*, 507–512.
- (32) Guo, Q.; Xu, C.; Yang, W.; Ren, Z.; Ma, Z.; Dai, D.; Minton, T. K.; Yang, X. *J. Phys. Chem. C* **2013**, *117*, 5293–5300.
- (33) He, Y.; Dulub, O.; Cheng, H.; Selloni, A.; Diebold, U. *Phys. Rev. Lett.* **2009**, *102*, 106105.
- (34) Wang, C.-Y.; Groenzin, H.; Shultz, M. J. *J. Phys. Chem. B* **2004**, *108*, 265–272.